Effect of Diffuseness Parameter on the Fusion Cross-Section of Closed-Shell Nuclei

Bilal M. Othman

Department of Physics/ College of Science/ University of Halabja/ Kurdistan Region/ Iraq

Adil M. Hussein

Department of Physics/ College of Science/ University of Sulaimani/ Kurdistan Region/ Iraq

Ali H. Taqi

Department of Physics/ College of Science/ University of Kirkuk/ Iraq
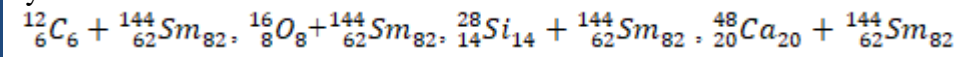
corresponding author:
Ali H. Taqi
alitaqi@uokirkuk.edu.iq

ABSTRACT

Heavy-ion fusion reactions are important and essential to express the dynamical properties of colliding nuclei, and to address the tunneling effect in quantum mechanics. In the fusion process, the ion-ion potential plays an important role in approaching the measured cross section with the experimental value by influencing the tunneling probability of interacting nuclei. In this work, the fusion cross-sections of closed-shell heavy-ion fusion systems

$$^{12}_{6}C_{6} + {}^{144}_{62}Sm_{82},\ {}^{16}_{8}O_{8} + {}^{144}_{62}Sm_{82},\ {}^{28}_{14}Si_{14} + {}^{144}_{62}Sm_{82},\ {}^{48}_{20}Ca_{20} + {}^{144}_{62}Sm_{82}$$

have been calculated and analyzed in the framework of coupled channel theory, using the code CCFULL, by fixing the potential depth value V_0= 102.9 MeV and the fusion radius R_0 = 1.096 fm, while, the diffuseness parameter (a_0) of Wood--Saxon potential is varied from 0.6 to 1.1 fm to fitting the fusion cross-section data at energies near and below the Coulomb barrier. It was observed that our approach is able to estimating the experimentally observed cross-sections of closed-shell colliding nuclei.

Keywords: Heavy-ion fusion, Diffuseness parameter, CCFULL code.

INTRODUCTION

Fusion is a reaction where two separate nuclei combine together to form a composite system. When the incident energy is not so large and the system is not so light, the reaction process is predominantly governed by quantum tunneling over the Coulomb barrier created by the strong cancellation between the repulsive Coulomb force and the attractive nuclear interaction. According to the developments in experimental techniques, fusion cross sections can now become measured for heavy-ion sub-barrier fusion reactions with high accuracy.

Theoretical heavy-ion fusion is the best scenario to express the dynamical properties of colliding nuclei and hence to result in new products such as compound nuclei, prediction of new heavy nuclei isotopes, and synthesis of superheavy elements. Over the last few decades, the nuclear structure served the heavy-ion fusion reactions significantly (Beckerman, 1988; Dasgupta *et al.*, 1998).

Coupled channels represent the approach and successful method for fusion (colliding) of two nuclei. It is now widely accepted that coupled-channel calculations for the heavy-ion reaction at energies close to and below the Coulomb barrier can explain the experimental results of fusion reactions of medium-heavy mass systems, heavy mass systems, and very heavy mass systems (Hagino and Takigawa, 2012; Back *et al.*, 2014)

The cross-section and barrier distribution for fusion reactions of the spherical nuclei are shown to be highly dependent on the structure of the interacting nuclei, the orientation of the two nuclear systems, and collective excitations (rotations and surface vibrations) (Timmers *et al.*, 1995; Hagino and Rowley, 2004).

The theoretical study specified by prediction or reproduction of the experimental data using a mathematical method such as either expanding or reformulating coupled channel equation, and truncating a huge matrix element to approach the calculated result of a certain model (for example Wong formula, cross-section equation barrier distribution equation, etc.) from the experimental one such as cross-section and the barrier distribution (Gautam, 2015).

There are several types of nuclear potentials; the Wood-Saxon (W.S) potential is successful in employing the heavy ion fusion. It includes coupling radius (R_o), surface diffuseness (a_0), and potential constant (V_0) which is used to reproduce experimental data (Gautam, 2015). Given below is the phenomenological W.S potential, which is adopted for the nuclear potential and often used to characterize various types of fusing ion interactions (Hagino *et al.*, 2005):

$$V(r) = \frac{V_0}{1+\exp\left[(r-R_0)/a_0\right]}; \quad R = r_o\left(A_P^{1/3} + A_T^{1/3}\right) \tag{1}$$

Here r is the distance between the center of mass of the projectile nucleus with the mass number A_P and that of the target nucleus with the mass number A_T (Newton *et al.*, 2004; Mukherjee *et al.*, 2007).

In this work, the theoretical calculations are performed using the Wong formula, formulated from the coupled-channels equations, for different fusion reactions, i.e., $^{12}_{6}C$, $^{16}_{8}O$, $^{28}_{14}Si$ and $^{48}_{20}Ca + ^{144}_{62}Sm$. In these reactions, these different closed-shell projectile nuclei are fused with the same target ($^{144}_{62}Sm$). The calculated values of these fusions are compared with experimental data. The calculations were implemented using the coupled channel (CCFULL) code (Hagino *et al.*, 1999), and by fixing the potential depth value $V_0 = 102.9$ MeV and the fusion radius $R_0 = 1.096$ fm. The diffuseness parameter (a_0) of Wood--Saxon potential is varied from 0.6 to 1.1 fm to fitting the fusion cross-section data at energies near and below the Coulomb barrier.

Coupled-channel model

To calculate the effects of coupling between relative motion of projectile-target and intrinsic degrees of freedom of them, using the set of diagonalizing Hamiltonian equations represent as the coupled channel equations given below:

$$\left[-\frac{\hbar^2}{2\mu}\frac{d^2}{dr^2} + -\frac{\hbar^2 J(J+1)}{2\mu r^2} + V(r) - E + \epsilon_n\right] u_n^J(r) = -\sum_{\acute{n}}\langle n|V_{coup}|\acute{n}\rangle\, u_{\acute{n}}^J(r) \qquad (2)$$

where n refers to a certain quantum state, J is the total angular momentum, The radial component of the entire wave function of coupled channels equations, and r is the radial coordinate for the relative motion between projectile-target nuclei. μ is the reduced mass of the fusing nuclei, E is the bombarding energy in the center of the mass frame, ϵ_n is the excitation energy of the n_{th} channel, $\langle n|V_{coup}|\acute{n}\rangle$ is the matrix elements of the coupling Hamiltonian and $u_{\acute{n}}^J(r)$ represent the radial component of the entire wave function of the system. The CCFULL code is employed to calculate the coupled-channel equations, wherein the coupled-channel equations are solved using the Numerov method and simplified by using the incoming wave boundary condition (IWBC) to diagonalizing eq. (2). This simplification called Potential Model (Hagino *et al*., 1999). Once the transmission coefficients T_{nn}^J are obtained, the inclusive penetrability of the Coulomb potential barrier is given by:

$$P_J(E) = 1 - |S_J|^2 = \sum_n |T_{nn'}^J|^2 \qquad (3)$$

The fusion cross section formulated from the Potential Model is given by (Takigawa *et al*., 2003; Jiang *et al*., 2021).

$$\sigma_F(E) = \frac{\pi}{\kappa^2}\sum_J(2J + 1)P_J(E) \qquad (4)$$

For vibrational coupling, the operator $\hat{O}_{Vib}$ in the nuclear coupling Hamiltonian is given by (Hagino *et al*., 1999), $\hat{O}_{Vib} = \frac{\beta_\lambda}{\sqrt{4\pi}}R_T\left(a_{\lambda 0}^\dagger + a_{\lambda 0}\right)$, where $a_{\lambda 0}^\dagger(a_{\lambda 0})$ is the creation (annihilation) operator of the phonon of the vibrational mode of multipolarity λ. The operator implanted in the nuclear coupling potential to take the matrix elements form as given,

$$V_{nm}^{(N)} = \langle n|V_N(r,\hat{O})|m\rangle - V_N^0\, \delta_{n,m} \qquad (5)$$

The matrix element of the $\hat{O}_{Vib}$ is located between the n-phonon state $|n\rangle$ and the m-phonon state $|m\rangle$, which are given by,

$$\hat{O}_{Vib(nm)} = \frac{\beta_\lambda}{\sqrt{4\pi}}R_T\left(\delta_{n,m-1}\sqrt{m} + \delta_{n,m+1}\sqrt{n}\right) \qquad (6)$$

The vibration Coulomb coupling matrix elements is given by (Hagino *et al*., 1999),

$$V_{nm}^{(C)} = \frac{\beta_\lambda}{\sqrt{4\pi}}\frac{3}{2\lambda+1}Z_P Z_T e^2\frac{R_T^\lambda}{r^{\lambda+1}}\left(\sqrt{m}\delta_{n,m-1} + \sqrt{n}\delta_{n,m+1}\right) \qquad (7)$$

The total coupling matrix elements are evaluated by taking the sum of $V_{nm}^{(N)}$ and $V_{nm}^{(C)}$.

RESULT AND DISCUSSION

The calculations have been performed for the fusion excitation functions of some closed shell heavy-ion systems. Using the Woods-Saxon (W.S) potential employed by the coupled-channel equation, that is associated with Wong's formula (Newton *et al*., 2004; Montagnoli and Stefanini, 2017; Gautam *et al*., 2019; Jiang *et al*., 2021; Cinan *et al*., 2021), implemented by the CCFULL code (Hagino *et al*., 1999). All projectiles ($^{12}_{6}C$, $^{16}_{8}O$, $^{28}_{14}Si$) and the target $^{144}_{62}Sm$ are either closed shell or closed sub-shell nuclei, some nuclei including magic and double magic numbers as shown in (Table 1). Closed shell nuclei have a systematic behavior at low-lying surface vibrational states about their equilibrium shape. It can be used to investigate the exciting function of the new fusion

system, such as $^{48}_{20}Ca + ^{144}_{62}Sm$. Thereby, compound nuclei obtain directly from the closed shell nuclei fusions, as recorded in the (Table 2). (Qu *et al.*, 2014).

Table 1: Target and projectiles configuration

| Target nucleus	Proton number	Neutron number	Type
$^{12}_{6}C$	6 ($1p_{2/3}$)	6 ($1p_{3/2}$)	Closed shell
$^{16}_{8}O$	8 ($1p_{1/2}$)	8 ($1p_{1/2}$)	Double magic number
$^{28}_{14}Si$	14 ($1d_{5/2}$)	14 ($1d_{5/2}$)	Closed shell
$^{48}_{20}Ca$	20 ($1d_{3/2}$)	28 ($1f_{7/2}$)	Double magic number
$^{144}_{62}Sm$	62 ($2d_{5/2}$)	82 ($1h_{11/2}$)	Magic number

There are two vibrational modes of excitations in the target nucleus $^{144}_{62}Sm$. A typical example is the quadrupole and octupole vibrational excitations, where $\beta_2 = 0.112$ for the state 2⁻ (1.66 MeV), and $\beta_3 = 0.206$, for the state 3⁻ (1.81 MeV) (Hagino *et al.*, 1997; Kuzyakin *et al.*, 2013; Kaur *et al.*, 2016; Denisov and Sedykh, 2019; Sargsyan *et al.*, 2011).

In the present work, the fusion cross-sections of $^{12}_{6}C$, $^{16}_{8}O$, $^{28}_{14}Si$, $^{48}_{20}Ca + ^{144}_{62}Sm$ systems have been calculated by fixing the potential depth value $V_0 = 102.9$ MeV and the fusion radius $R_0 = 1.096$ fm, while the diffuseness parameter (a_0) of W.S potential are varied from 0.6 to 1.1 fm to fitting the fusion cross-section data. The best agreements were at the values of Table 2, other studies have been carried in a_0 variation method (Newton *et al.*, 2001; Hagino *et al.*, 2003; Zamrun and Greiner, 2008; Zamrun, 2016; Najim *et al.*, 2019).

Table 2: The optimized values of the diffuseness parameters a_0 (fm) of the nuclear potential, companies by fixed values of the potential depth $V_0 = 102.9$ MeV and the fusion range $R_0 = 1.096$ fm, and the compound nucleus (Nuclear Data Services, 2022), for the listed fusion systems.

Fusion Reaction	$a_0(fm)$ present work	Compound nucleus
$^{12}_{6}C + ^{144}_{62}Sm$	0.60	$^{156}_{68}Er$
$^{16}_{8}O + ^{144}_{62}Sm$	0.77	$^{160}_{70}Yb$
$^{28}_{14}Si + ^{144}_{62}Sm$	0.97	$^{172}_{76}Os$
$^{48}_{20}Ca + ^{144}_{62}Sm$	------	$^{192}_{82}Pb$

In Fig. (1), we calculated the cross-section of the $^{12}_{6}C + ^{144}_{62}Sm$ fusion. Both projectile and target are closed-shell nuclei and recognize only by low-lying surface vibrational states as the essential mode of couplings. For a study of coupling in CCFULL calculations, we selected the Ec. m values ranging from 40 MeV to 90 MeV. The projectile coupled to the one phonon 3⁻ and 2⁺ vibrational states of the target $^{144}_{62}Sm$. The results are also compared with the non-coupled fusion. The $^{12}_{6}C + ^{144}_{62}Sm$ fusion cross-section was calculated using other theoretical methods (Janssens *et al.*, 1986; Denisov and Sedykh, 2019).
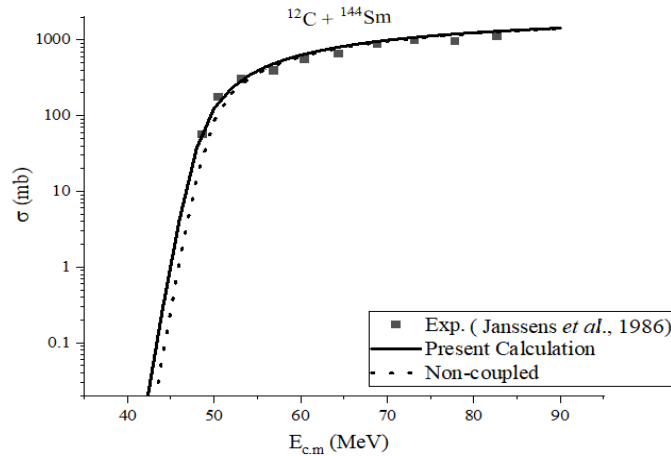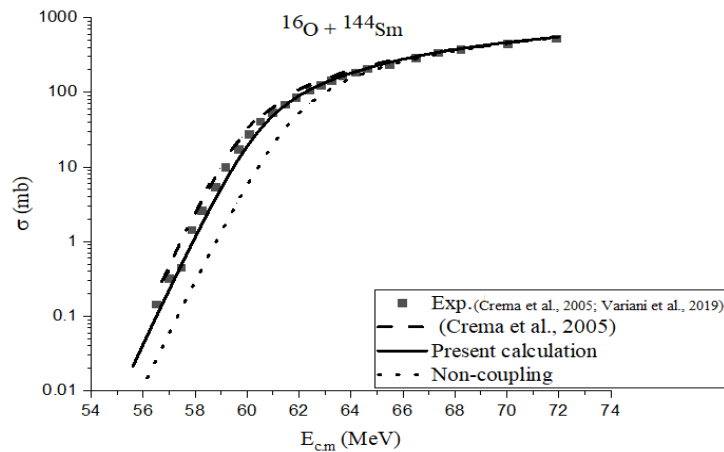
Fig. 1: The fusion cross-section of $^{16}_{8}C + ^{144}_{62}Sm$ reaction. The solid-line represents the coupled case with $a_0 = 0.60\ fm$. The dotted-line is non-coupled case, and the square symbols represent the experimental data, which was taken from ref. (Janssens et al., 1986).

Our results are in a good agreement with the experimental data with the diffuseness parameter $a_0 = 0.60\ fm$ as depicted in Fig. (1) and it is better than the non-coupled calculations in describing data.

Fig. (2) shows the experimental data compared to both calculated and non-coupled data of the cross-section $^{16}_{8}O + ^{144}_{62}Sm$ fusion, where the projectile is taken to be inert and the diffuseness parameter $a_0 = 0.77\ fm$. The cross section $^{16}_{8}O + ^{144}_{62}Sm$ fusion has been strongly influenced at below barrier energies by the low-lying surface vibrations and spherical shape of the $^{144}_{62}Sm$ target (Gautam et al., 2017), this method can be found in Ref. (Iwamoto and Moller, 1996).

From Fig. (2), we observed that our presented calculations are better than the non-coupled (inert target) calculations in reproducing data, due to the strength of the octupole vibrational state of $^{144}_{62}Sm$ target. Fig. (2) clarified that the experimental data is slightly underestimated by the calculations performed by E. Crema et al. (Crema et al., 2005). Thereby, the present results are also consistent to those recorded in the previous studies (Crema et al., 2005; Denisov and Sedykh, 2019; Variani et al., 2019).

Fig. 2: Different calculations for the fusion cross-section of $^{16}_{8}O + ^{144}_{62}Sm$ reaction. The solid-line represent the presents calculations with $a_0 = 0.77\ fm$, the dotted-line is no-coupled case and dashed-line is the calculations of Ref. (Crema et al., 2005), and the square symbols indicate the experimental data, which was taken from ref. (Crema et al., 2005; Variani et al., 2019).

Fig. (3) clarifies the calculated fusion cross-section of the $^{28}_{14}Si + {}^{144}_{62}Sm$, with $a_0 = 0.99\ fm$, as tabulated in (Table 2). Our calculated cross sections do not agree with the experimental data, exactly in the low $E_{c.m}$ region. This deficient return to the inclusion of the rotational states in $^{28}_{14}Si$ as well as the 2^+ and 3^- vibrational states in $^{144}_{62}Sm$ (Gautam *et al*., 2020). Further, we selected the inert case for the projectile ($^{28}_{14}Si$). This selection works well for heavy nuclei where the excitation energies of the rotational band are small, while the $^{28}_{14}Si$ nucleus has a large ground state rotational quadrupole deformation of $\beta_2 = -0.4$ (Baby *et al*., 2000). To our knowledge, there are no theoretical results using CCFULL code that have a better agreement with the experiential data, but there is an empirical method extracted from the experimental data so-called universal fusion function (UFF), that was used by V.V Sargsyan (Sargsyan *et al*., 2011), as shown in Fig. (3). (Dasgupta *et al*., 1998; Montagnoli and Stefanini, 2017; Gautam *et al*., 2020).

The $^{48}_{20}Ca + {}^{144}_{62}Sm$ fusion does not have experimental data. We propose the new method for calculating the cross-section of $^{48}_{20}Ca + {}^{144}_{62}Sm$ by predicting the value for diffuseness parameter a_0, while the values of V_0 and r_0 remain constant. This is done by extracting the new value of the a_0 from the graph between the diffuseness parameters of the different mentioned fusion systems and the mass number of the projectile nuclei (A_p) as shown in Fig. (4).
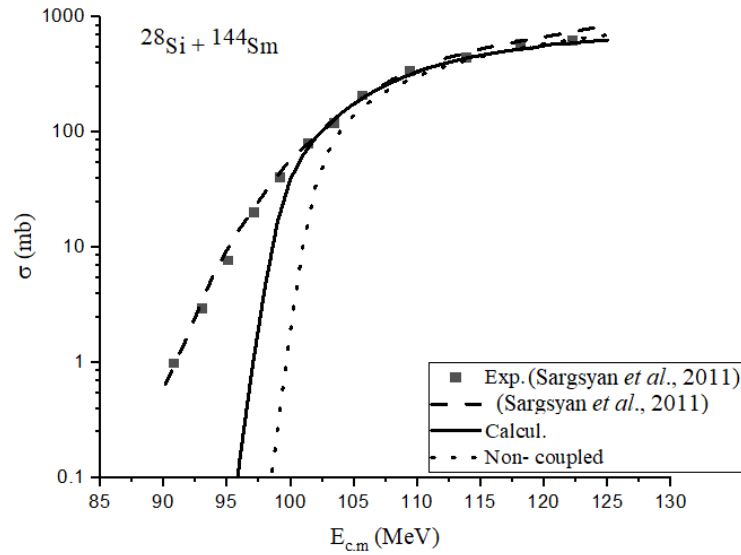
Fig. 3: Different calculation for the fusion cross-section of $^{28}_{14}Si + {}^{144}_{62}Sm$ reaction. The solid-line represents the present calculations with $a_0 = 0.99\ fm$, the dotted-line is non-coupled case, the dashed-line is the empirical results of V.V Sargsyan (Sargsyan *et al*., 2011), and the square symbols indicate the experimental data, which was taken from ref. (Sargsyan *et al*., 2011).

Since the $^{48}_{20}Ca + {}^{144}_{62}Sm$ fusion does not have experimental data, in this work, we estimate the value of a_0 by fitting the obtained values of diffuseness parameter (a_0) values (of $^{12}_{6}C$, $^{16}_{8}O$ and $^{28}_{14}Si + {}^{144}_{62}Sm$ systems) to the mass number of the projectile nuclei (A_p) as shown in Fig. (4), we have found the following formula:

$$a_0(A_p) = 1.079 - 1.691e^{-0.105\,A_p} \qquad (9)$$
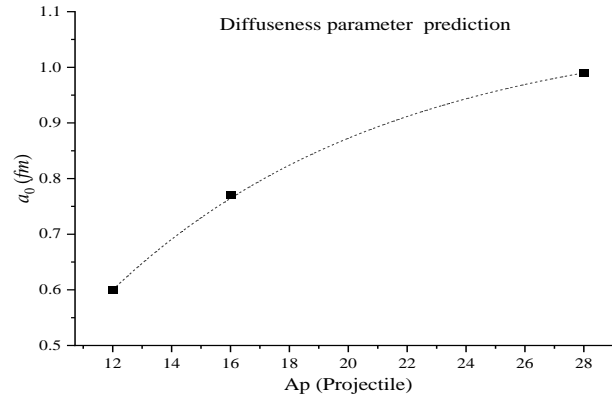
Fig. 4: diffuseness parameter a_0 vs. Mass number of the projectile nuclei (A_p) for $^{12}_{6}C$, $^{16}_{8}O$ and $^{28}_{14}Si+ {^{144}_{62}Sm}$ fusion systems.

From eq. (9), we obtained the value of $a_0 = 1.068\ fm$ for the $^{48}_{20}Ca + {^{144}_{62}}\ Sm$. Fig. (5) shows our cross-section calculations (solid-line) of $^{48}_{20}Ca + {^{144}_{62}}Sm$ in comparison with each of the present calculations (dash-line) and the experimental data (closed squares) (Stefanini *et al.*, 2005) of the $^{48}_{20}Ca + {^{154}_{62}}Sm$ reactions. We selected the rotational band for both the projectile and the target. The $^{48}_{20}Ca$ band specified by $\beta_2 = 0.105$ for the state 2^+ (3.831MeV), and the $^{144}_{62}Sm$ band with $\beta_2 = 0.11$, for the state 2^- (1.66 MeV). Our calculated cross sections have not convenient well with the capture experimental data, exactly in the low $E_{c.m}$ region. The reason for shortcoming the present calculated fusion cross-section of the $^{48}_{20}Ca + {^{144}_{62}}\ Sm$ reaction return to the fact that the captured cross section data always greater than the fusion data 7 (Zagrebaev, 2004; Trotta *et al.*, 2005; Knyazheva *et al.*, 2007; Mandaglio *et al.*, 2009). Thereby, the projectile $^{48}_{20}Ca$ nucleus coupling to rotational states and neutron rich nuclei channels of the target isotopes $^{154}_{62}Sm$ lead to significantly larger fusion cross-sections than the low line vibrational states of the spherical target $^{144}_{62}Sm$ (Knyazheva *et al.*, 2007; Wang *et al.*, 2007; Sargsyan *et al.*, 2011; Montagnoli and Stefanini, 2017; Gautam *et al.*, 2017; Denisov and Sedykh, 2019).
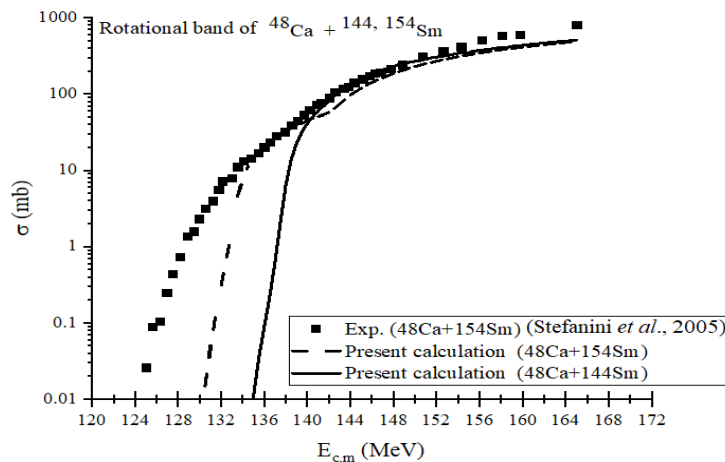
Fig. 5: Calculations of the $^{48}_{20}Ca + {^{144}_{62}}\ Sm$ and $^{48}_{20}Ca + {^{154}_{62}}\ Sm$ reactions with the experimental data of the $^{48}_{20}Ca + {^{154}_{62}}Sm$ fusion. The dash-line represent the presents calculations of the $^{48}_{20}Ca + {^{154}_{62}}\ Sm$ with $a_0 = 1.068\ fm$. The solid-line is the presents calculations of the $^{48}_{20}Ca + {^{144}_{62}}\ Sm$ with $a_0 = 1.068\ fm$. The square symbols represent the experimental data of the capture fusion of the $^{48}_{20}Ca + {^{154}_{62}}Sm$ reaction (Stefanini *et al.*, 2005).

In particular, $^{48}_{20}Ca$ has the significant difference. This is due to the well-known shape change when going from $^{12}_{6}C$ (spherical) to $^{48}_{20}Ca$ having a stable (intrinsic) prolate deformation. It specified by high fusion Q-value (Qu *et al.*, 2014), and thick neutron skin (Matsuzaki and Yahiro, 2022) if compared with the $^{12}_{6}C$ and $^{16}_{8}O$ projectiles. In contrast, the $^{28}_{14}Si$ projectile has a large ground state rotational quadrupole deformation of $\beta_2 = -0.4$ (Baby *et al.*, 2000) too. Maybe this structural information plays the main role in falling down the crosse-section values below of the barrier region for each of the $^{48}_{20}Ca + ^{144}_{62}Sm$ and $^{28}_{14}Si + ^{144}_{62}Sm$ fusion reactions, as shown in Figs. (3, 5).

CONCLUSIONS

This study deal with the fusion of some closed shell ($^{12}_{6}C$, $^{16}_{8}O$, $^{28}_{14}Si$, $^{48}_{20}Ca$) projectile, each one of them collides separately with the same target nucleus ($^{144}_{62}Sm$) to calculate the cross-section. Using the CCFULL code to solve the coupled-channel equations for different fusion reactions, such as $^{12}_{6}C$, $^{16}_{8}O$, $^{28}_{14}Si$, $^{48}_{20}Ca + ^{144}_{62}Sm$ systems. The results show that the CCFULL code is successful in approaching the calculated results to the experimental data.

The calculated fusion cross-section of the light mass ($^{12}_{6}C$, $^{16}_{8}O$) projectile with $^{144}_{62}Sm$ target coincide with experimental data. This coincide used for determining the cross-section values of the two fusion types (evaporation residue and total fusion) of the $^{12}_{6}C + ^{144}_{62}Sm$ fusion. The same result was investigated in the previous study (Janssens *et al.*, 1986). However, for medium nuclei ($^{28}_{14}Si$, $^{48}_{20}Ca$) there are not in agreement in the low $E_{c.m}$ region.

The systematic variation of the projectiles leads to yielding the compound nuclei directly from the mentioned fusions, as recorded in (Table 2). Further, the authors planned to determine the product (evaporation residue, fission-fusion, etc.) types of the calculated fusion reactions in a future study.

In this work, we focused on the surface diffuseness parameters' impact on the fusion cross sections. In addition, we studied the relation between the diffuseness parameters and the projectile atomic mass numbers. We estimated that the diffuseness parameter for closed-shell (double magic) nuclei undergoes regular variation as shown in Fig. (4). The relation is used for finding a new diffuseness parameter. Wherein, the new parameter $a_0 = 1.068 \, fm$. It is also employed to predict the new result for $^{48}_{20}Ca + ^{144}_{62}Sm$ fusion using the CCFULL code, which does not have experimental data. We deeply discussed that the calculated cross-section data of the $^{48}_{20}Ca + ^{144}_{62}Sm$ reaction is close to the exact data, as shown in Fig. (5).

ACKNOWLEDGMENTS

Declaration of Competing Interest
The authors declare no conflict of interest.

REFERENCES

Baby, L.T.; Tripathi, V.; Das, J.J.; Sugathan, P.; Madhavan, N.; Sinha, A.K.; Radhakrishna, M.C.; Madhusudhana Rao, P. V.; Hui, S. K.; Hagino, K. (2000). Role of 28Si excitations in the sub-barrier fusion of 28Si+120Sn. *Phys. Rev. C,* **62**(1), 014603.

Back, B.B.; Esbensen, H.; Jiang, C.L.; Rehm, K.E. (2014). Recent developments in heavy-ion fusion reactions. *Revi. Modern Phys.,* **86**(1), 317-360.

Beckerman, M. (1988). Sub-barrier fusion of two nuclei. *Reports on Progress in Phys.,* **51**(8), 044610-1- 044610-7.

Cinan, Z.M.; Erol, B.; Baskan, T.; Yilmaz, A.H. (2021). Heavy-ion fusion reaction calculations: establishing the theoretical frameworks for 111in radionuclide over the coupled channel model. *Energ.,* **14**(24), 8594.

Crema, E.; Chamon, L.C.; Gomes, P.R.S. (2005). Reliable potential for studying fusion of weakly bound nuclei. *Phys. Rev. C,* **72**, 034610.

Dasgupta, M.; Hinde, D.J.; Rowley, N.; Stefanini, A.M. (1998). Measuring barriers to fusion. *Annual Rev.,* **48**, 401-461.

Denisov, V.Yu.; Sedykh, I.Yu. (2019). Empirical relations for the fusion cross sections of heavy ions. *European Phys. J. A,* **55**(153).

Gautam, M.S. (2014). Role of neutron transfer in the enhancement of sub-barrier fusion excitation functions of various systems using an energy-dependent Woods-Saxon potential. *Phys. Rev. C,* **90**(2), 024620.

Gautam, M.S. (2015). Effects of intrinsic degrees of freedom in enhancement of sub-barrier fusion excitation function data. *Modern Phys. Lett. A,* **30**(6), 1550013.

Gautam, M.S. (2015). Systematic failure of static nucleus–nucleus potential to explore sub-barrier fusion dynamics. *Phys. Scr.,* **5**(055301), 90.

Gautam, M.S.; Khatri, H.; Vinod, K. (2019). Interplay of neutron transfer and collective degrees of freedom in the fusion dynamics of 16O+76Ge and 18O+74Ge reactions. *International J. Modern Phys. E,* **28**(1-2), 1950006.

Gautam, M.S.; Vinod, K.; Kumar, H. (2017). Role of barrier modification and nuclear structure effects in sub-barrier fusion dynamics of various heavy ion fusion reactions. *Brazilian J. Phys.,* **47**, 461–472.

Gautam, M.S.; Duhan, U.; Chahal, R.P.; Khatri, H.; Kuhar, S.B.; Vinod, K. (2020). Influence of neutron transfer channels and collective excitations in the fusion of 28Si with 90,92,94,96Zr targets. *Phys. Rev.C,* **102**(1), 014614.

Hagino, K.; Balantekin, A.B. (2004). WKB approximation for multichannel barrier penetrability. *Phys. Rev. A,* **70**(3), 032106.

Hagino, K.; Rowley, N. (2004). Large-Angle scattering and quasielastic barrier. *Phys. Rev. C,* **69**, 054610.

Hagino, K.; Rowley, N.; Dasgupta, M. (2003). Fusion cross sections at deep sub-barrier energies. *Phys. Rev. C,* **67**(5), 054603.

Hagino, K.; Rowley, N.; Kruppa, A.T. (1999). A program for coupled-channel calculations with all order couplings for heavy-ion fusion reactions. *Computer Phys. Communicat.,* **123**(1-3), 143-152.

Hagino, K.; Takehi, T.; Balantekin, A.B.; Takigawa, N. (2005). Surface diffuseness anomaly in heavy-ion potentials for largeangle quasielastic scattering. *Phys. Rev. C,* **71**, 044612.

Hagino, K.; Takigawa, N. (2012). Subbarrier fusion reactions and many-particle quantum tunneling. *Progress of Theoret. Phys.,* **128**(6), 1061–1106.

Hagino, K.; Takigawa, N.; Kuyucak, S. (1997). Role of anharmonicities of nuclear vibrations in fusion reactions at sub-barrier energies. *Phys. Rev. Lett.,* **79**(16), 2943.

Iwamoto, A.; Moller, P. (1996). Nuclear deformation and sub-barrier fusion cross sections. *Nucl. Phys. A,* **605**, 334-358.

Janssens, R.V.F.; Holzmann, R.; Henning, W.; Khoo, T.L.; Lesko, K.T.; Stephans, G.S.F.; Radford, D.C.; Van Den Berg, A.M.; Kühn, W.; Ronningen, R.M. (1986). Evaporation residue cross sections and average neutron multiplicities in the 64Ni+92Zr and 12C+144Sm reactions leading to 156Er. *Phys. Lett. B,* **181**(1-2), 16-20.

Jiang, C.L.; Back, B.B.; Rehm, K.E.; Hagino, K.; Montagnoli, G.; Stefanini, A.M. (2021). Heavy-ion fusion reactions at extreme sub-barrier energies. *European Phys. J. A, (EPJ A),* **57**, 47.

Kaur, G.; Behera, B.R.; Jhingan, A.; Nayak, B.K.; Dubey, R.; Sharma, P.; Thakur, M.; Mahajan, R.; Saneesh, N.; Khushboo, T. B.; Kumar, A.; Mandal, S.; Saxena, A.; Sugathan, P.;

Rowley, N. (2016). Effect of coupling in the 28Si + 154Sm reaction studied by quasi-elastic scattering. *Phys. Rev., C,* **94**, 034613.

Knyazheva, G.N.; Kozulin, E.M.; Sagaidak, R.N.; Chizhov, A.Yu.; Itkis, M.G.; Kondratiev, N.A.; Voskressensky, V.M.; Stefanini, A.M.; Behera, B.R.; Corradi, L.; Fioretto, E.; Gadea, A.; Latina, A.; Szilner, S.; Trotta, M.; Beghini, S.; Montagnoli, G. (2007). Quasifission processes in 40,48Ca+144,154Sm reactions. *Phys. Rev. C,* **75**(6), 064602.

Knyazheva, G.N.; Kozulin, E.M.; Sagaidak, R.N.; Chizhov, A. Yu.; Itkis, M. G.; Kondratiev, N. A.; Voskressensky, V.M.; Stefanini, A.M.; Behera, B. R.; Corradi, L.; Fioretto, E.; Gadea, A.; Latina, A.; Szilner, S.; Trotta, M.; Beghini, S.; Montagnoli, G. (2007). Quasifission processes in 40,48Ca+144,154Sm reactions. *Phys. Rev. C,* **75**(6), 064602.

Kuzyakin, R.A.; Sargsyan, V.V.; Adamian, G.G.; Antonenko, N.V. (2013). Study of isotopic effects in capture process. *Acta Phys. Polon. B,* **44**(3), 471.

Mandaglio, G.; Fazio, G.; Giardina, G.; Hanappe, F.; Manganaro, M.; Muminov, A. I.; Nasirov, A. K.; Saccá, C. (2009). Investigation of the role of the projectile-target orientation angles on the evaporation residue production. *Phys. Atom. Nucl.,* **72**, 1639-1650.

Matsuzaki, M.; Yahiro, M. (2022). Neutron skin of 48Ca deduced from interaction cross-section. *Modern Phys. Lett. A,* **37**(19), 2250123.

Montagnoli, G.; Stefanini, A.M. (2017). Recent experimental results in sub- and near-barrier heavy ion fusion reactions. *European Phys. J. A,* **53**.

Mukherjee, A.; Hinde, D.J.; Dasgupta, M.; Hagino, K.; Newton, J.O.; Butt, R.D. (2007). Failure of the Woods–Saxon nuclear potential to simultaneously reproduce precise fusion and elastic scattering measurements. *Phys. Rev. C,* **75**, 044608.

Najim, A.J.; Majeed, F.A.; Al-Attiyah, K.H. (2019). Improved calculation of fusion barrier distribution. *IOP Conf. Ser.: Mater. Sci. and Engineer.,* **571**, 012124.

Newton, J.O.; Morton, C.R.; Dasgupta, M.; Leigh, J.R.J.; Mein, C.; Hinde, D.J.; Timmers, H.; Hagino, K. (2001). Experimental barrier distributions for the fusion of 12C, 16O, 28Si, and 35Cl with 92Zr and coupled-channels analyses. *Phys. Rev. C,* **64**(6), 64 064608-1, _064608-12.

Newton, J.O.; Butt, R.D.; Dasgupta, M.; Hinde, D.J.; Gontchar, I.I.; Morton, C.R.; Hagino, K. (2004). Systematic failure of the Woods-Saxon nuclear potential to describe both fusion and elastic scattering: Possible need for a new dynamical approach to fusion. *Phys. Rev. C,* **70**, 70 024605-1,70 024605-15.

Newton, J.O.; Butt, R.D.; Dasgupta, M.; Hinde, D.J.; Gontchar, I.I.; Morton, C.R.; Hagino, K. (2004). Systematics of precise nuclear fusion cross sections: the need for a new dynamical treatment of fusion?. *Phys. Lett. B,* **586**(3-4), 219-224.

Nuclear Data Services, provided by the Nuclear Data Section.(2022). "International Atomic Energy Agency." *Available at https://www.nndc.bnl.gov/qcalc/..*

Qu, W.W.; Zhang, G.L.; Zhang, H.Q.; Wolski, R. (2014). Comparative studies of Coulomb barrier heights for nuclear models applied to sub-barrier fusion. *Phys. Rev. C,* **90**(6), 064603.

Sargsyan, V.V.; Adamian, G.G.; Antonenko, N.V.; Scheid, W.; Zhang, H.Q. (2011). Effects of nuclear deformation and neutron transfer in capture processes, and fusion hindrance at deep sub-barrier energies. *Phys. Rev.,* **84**, 064614.

Stefanini, A.M.; Trotta, M.; Behera, B.R.; Corradi, L.; Fioretto, E.; Gadea, A.; Latina, A.; Szilner, S.; Wu, Y.W.; Beghini, S.; Montagnoli, G.; Scarlassara, F.; Chizhov, A. Yu.; Itkis, I.M.; Kondratiev, N.A.; Pokrovskiy, I.V.; Sagaidak, R.N.; Kniajeva, G.N. (2005). Fusion-evaporation cross-sections for 48Ca + 154Sm near the Coulomb barrier. *European Phys. J. A,* **23**, 473–480.

Takigawa, N.; Masamoto, T.; Takehi, T.; Rumin, T. (2003). Heavy ion fusion reactions and tunneling nuclear microscope. *J. Korean Phys. Soc.,* **41**(16), 91-99.

Timmers, H.; Leigh, J.R.; Dasgupta, M.; Hinde, D.J.; Lemmon, R.C.; Mein, J.C.; Morton, C.R.; Newton, J.O.; Rowley, N. (1995). Probing fusion barrier distributions with quasi-elastic scattering. *Nucl. Phys. A,* **584**(1), 190-204.

Trotta, M.; Stefanini, A.M.; Beghini, S.; Behera, B.R.; Chizhov, A.Yu.; Corradi, L.; Courtin, S.; Fioretto, E.; Gadea, A.; Gomes, P.R.S.; Haas, F.; Itkis, I.M.; Itkis, M.G.; Kniajeva, G. N.; Kondratiev, N.A.; Kozulin, E.M.; Latina, A.; Montagnol, G. (2005). Fusion hindrance and quasi-fission in 48Ca induced reactions. *European Phys. J. A,* **25**, 615–618.

Variani, V.I.; Usman, I.; Firihu, M.Z. (2019). Effects of surface diffuseness and coupling radius parameters on the fusion and quasi-elastic barrier distributions. *Indonesian J. Appl. Phys.,* **9**(1), 22-33.

Wang, N.; Li, Z.; Scheid, W. (2007). Systematic study of fusion barriers. *J. Phys. G: Nuclear and Particle Phys.,* **34**, 1935.

Wong, C. Y. (1973). Interaction barrier in charged-particle nuclear reactions. *Phys. Rev. Lett.,* **31**, (12), 766-769.

Zagrebaev, V.I. (2004). Fusion-fission dynamics of super-heavy element formation and decay. *AIP Confer. Proceed.,* **704**(1).

Zagrebaev, V.; Greiner, W. (2008). Synthesis of superheavy nuclei: A search for new production reactions. *Phys. Rev. C,* **78**(3), 034610.

Zamrun, M.F. (2016). Role of triple phonon excitations in large angle quasi-elastic scattering of very heavy mass systems. *Internat. J. Modern Phys. E,* **25**(8), 1650054-1-1650054-10.

تأثير معامل الانتشار على المقطع العرضي للاندماج في الانوية مغلقة الغلاف

عادل محمد حسين   **بلال محمد عثمان**

قسم الفيزياء/ كلية العلوم/ جامعة السليمانية   قسم الفيزياء/ كلية العلوم/ جامعة حلبجة

علي حسين تقي

قسم الفيزياء/ كلية العلوم/ جامعة كركوك

الملخص

تعتبر تفاعلات اندماج الأيونات الثقيلة مهمة وضرورية للتعبير عن الخصائص الديناميكية للانوية المتصادمة اضافة الى معالجة ظاهرة النفق الكمي tunneling effect. في عملية الاندماج، يلعب جهد الأيونات دورًا مهمًا في اقتراب المقطع العرضي المقاس من القيمة التجريبية من خلال تأثير احتمالية النفق الكمي على الانوية المتفاعلة. في هذا العمل، المقاطع العرضية لأنظمة الاندماج بين الانوية ذات الغلاف المغلق $^{12}_{6}C_{6} + ^{144}_{62}Sm_{82}$، $^{16}_{8}O_{8} + ^{144}_{62}Sm_{82}$، $^{28}_{14}Si_{14} + ^{144}_{62}Sm_{82}$، $^{48}_{20}Ca_{20} + ^{144}_{62}Sm_{82}$ تم حسابها وتحليلها في إطار نظرية القناة المقترنة coupled channel theory، باستخدام الكود CCFULL، عن طريق تثبيت قيمة العمق potential depth $V_0 = 102.9$ MeV ونصف قطر الاندماج fusion radius $R_0 = 1.096$ fm ، بينما تم تغيير قيم معامل الانتشار diffuseness parameter (a_0) في جهد Wood - Saxon من 0.6 fm إلى 1.1 لكي تتوائم القيم المحسوبة للمقطع العرضي للاندماج مع القيم العملية عند الطاقات القريبة والتي تقل عن حاجز كولوم. لقد لوحظ أن الاسلوب المستخدم في هذا العمل قادر على تقدير المقاطع العرضية لنوى الاصطدام مغلقة الغلاف.

الكلمات الدالة: اندماج الأيونات الثقيلة، معامل الانتشار، تفاعل كود CCFULL.